Orbital Hybridization and Charge Transfer in Carbon Nanopeapods

Youngmi Cho,[1] Seungwu Han,[2] Gunn Kim,[1] Hosik Lee,[1] and Jisoon Ihm[1,*]

[1]*School of Physics, Seoul National University, Seoul 151-747, Korea*
[2]*Princeton Materials Institute, Princeton University, Princeton, New Jersey 08544*
(Received 12 October 2002; published 14 March 2003)

We investigate the electronic structure of the fullerenes encapsulated inside carbon nanotubes, the so-called nanopeapods, using the first-principles study. The orbital hybridization of LUMO + 1 (the state above the lowest unoccupied molecular orbital) of C_{60}, rather than LUMO as previously proposed, with the nanotube states explains the peak at ~ 1 eV in recent scanning-tunneling-spectroscopy (STS) data. For the endohedral metallofullerenes nested in the strained nanotube, the charge transfer shifts the relative energy levels of the different states and produces a spatial modulation of the energy gap in agreement with another STS experiment.

The encapsulation of various kinds of molecules inside the carbon nanotube (CNT) by chemical or physical insertion methods [1] opened a new way to engineering the physical properties of the CNT. The acquired novel electronic and mechanical properties would be useful for practical applications. Recently, several groups have reported the observation of the single-walled nanotube with a chain of fullerenes inside, so-called carbon nanopeapods, through the high-resolution transmission electron microscopy or the electron diffraction pattern [2]. The encapsulation process is exothermic if the separation between the inserted fullerene and the wall of the nanotube is around the van der Waals distance (~ 3.3 Å). The fullerene bigger than this size can still be incorporated depending on environment, albeit endothermically [3].

In the recent scanning-tunneling-microscopy (STM) experiment on the nanopeapod [4,5], it was found that the fullerenes or metallofullerenes encapsulated in the single-walled semiconducting nanotube significantly affect the local electronic structure of the tube. For example, the STM image on C_{60}@CNT showed the modulation of the density of states (DOS) in the conduction band with the period of the underlying C_{60} array [4]. When C_{82} incorporating a gadolinium (Gd) atom is encapsulated [5], the band gap is found to decrease significantly at the location of C_{82}. In this Letter, we have carried out first-principles pseudopotential calculations for the carbon nanopeapods to understand the above experiments. Based on the simulated STM and scanning-tunneling-spectroscopy (STS) data, we show that the modification of the electronic structure of nanopeapods is explained in terms of the coupling strength between the fullerene and the CNT, charge transfer among constituents of the peapod, and the intermolecular distance between inserted fullerenes inside the nanotube. As the model systems for theoretical investigation, we choose C_{60}@(17, 0), C_{82}@(17, 0), and La@C_{82}@(17, 0) peapods. The semiconducting (17, 0) nanotube has the same diameter and the band gap as those used in experiment

[4,5], and its relatively small cell size is computationally manageable. Because of the computational difficulties in dealing with f-electrons in Gd with which the experiment in Ref. [5] was done, we replace Gd with an isovalent lanthanum (La) atom which would behave similarly to Gd in the present situation.

The first-principles pseudopotential calculations are carried out within the local density approximation using a plane-wave basis set [6]. The ultrasoft pseudopotentials [7] are employed with the cutoff energy of 25 Ry. For La, we treat all 11 valence electrons ($5s^2 5p^6 6s^2 5d^1$) explicitly since the $5s$ and $5p$ states cannot be considered to be frozen as core states [8]. The lateral (xy) dimension of the tetragonal supercell (with the nanotube axis along the z direction) is bigger than 20 Å which is large enough to avoid the intertube interaction. The fullerenes are repeated in the tube axis direction for every 12.7 Å to minimize the unit supercell size without causing an artificial strain on the system. The atomic coordinates are relaxed until the Hellmann-Feynman forces are reduced to within 0.05 eV/Å.

We first discuss the relaxed structures of the model peapods. In the C_{60}@(17, 0) peapod, the interwall separation between the nanotube and C_{60} is 3.2 Å which is close to the van der Waals distance, implying an exothermic encapsulation of C_{60}. Actually, the computed reaction energy [= E(peapod) − E(CNT) − E(fullerene)] is found to be −1.61 eV per unit cell which is similar to the reported value for C_{60}@(10, 10) [3]. In addition, there is practically no strain on any bonds in the nanotube or the fullerene. On the other hand, for the encapsulation of C_{82} whose diameter is ~ 8 Å (1 Å larger than that of C_{60}), the interwall distance between the nanotube and C_{82} after the atomic relaxation turns out to be 3.0 Å, 0.2 Å smaller than in the case of C_{60}, and the insertion is endothermic with the reaction energy of 0.16 eV per unit cell. Because of a tight embedding, the nanotube undergoes radial deformation around the fullerene, resulting in the maximum diametrical expansion of 0.5 Å. The bonds in the

circumferential direction (to be precise, 60° with respect to the tube axis) are then stretched up to 1% while the bonds parallel to the tube axis shrink up to 0.5%. This means that the insertion of an oversized fullerene corresponds to a local compressive stress along the tube axis. The reaction force from the tube exerts a tensile stress on C_{82} with the strain in the range between −2% and 4%.

Now we try to explain the experiment by Hornbaker *et al.* [4]. In Fig. 1, we present the simulated topographic STM image of $C_{60}@(17,0)$ evaluated at a plane located 5 Å above the surface of the nanotube. The STM images are obtained based upon the Tersoff-Hamann model [9]. The underlying atomic structure is shown in Fig. 1(a) and the STM images corresponding to sample biases of ±1.5 eV are presented in Figs. 1(b) and 1(c), respectively. The simulated image at −1.5 eV bias reveals only atomic corrugation of the CNT, and the presence of C_{60}'s inside the nanotube is not observable. Although the h_u states of C_{60} (the highest occupied molecular orbital of the isolated C_{60}) lies near −1.5 eV, they do not couple with the π states of the CNT due to the symmetry mismatch and contribute little to the electron tunneling current from the CNT to the STM tip. On the other hand, the image for the +1.5 eV bias in Fig. 2(c) shows the bright spots, i.e., higher tunneling currents, at the positions of C_{60}'s. These spots are originated from the hybridization of the t_{1g} states of C_{60} lying above the lowest unoccupied molecular orbital (LUMO) in energy (called the LUMO + 1) with the π or π^* states of the CNT. These simulated

images are in excellent agreement with the experimental topographic images in Figs. 1B and 1C of Ref. [4].

In Fig. 2(a), the computed DOS is shown for $C_{60}@(17,0)$. It can be seen that the t_{1u} band of C_{60} is the lowest conduction band of the peapod system. Because the separation between C_{60} and the nanotube wall (3.2 Å) is close to the van der Waals distance, there is no appreciable chemical bonding between them. A detailed analysis indicates that the charge transfer between C_{60} and the CNT is negligible here. In Fig. 2(b), the simulated dI/dV spectra are plotted at two feature locations, one at C_{60} and the other in the middle of two neighboring C_{60}'s (with the tip 5 Å above the tube wall) [10]. We stress here that the STS measures the tail of the wave function rather than the usual DOS at the atomic position. There is a peak
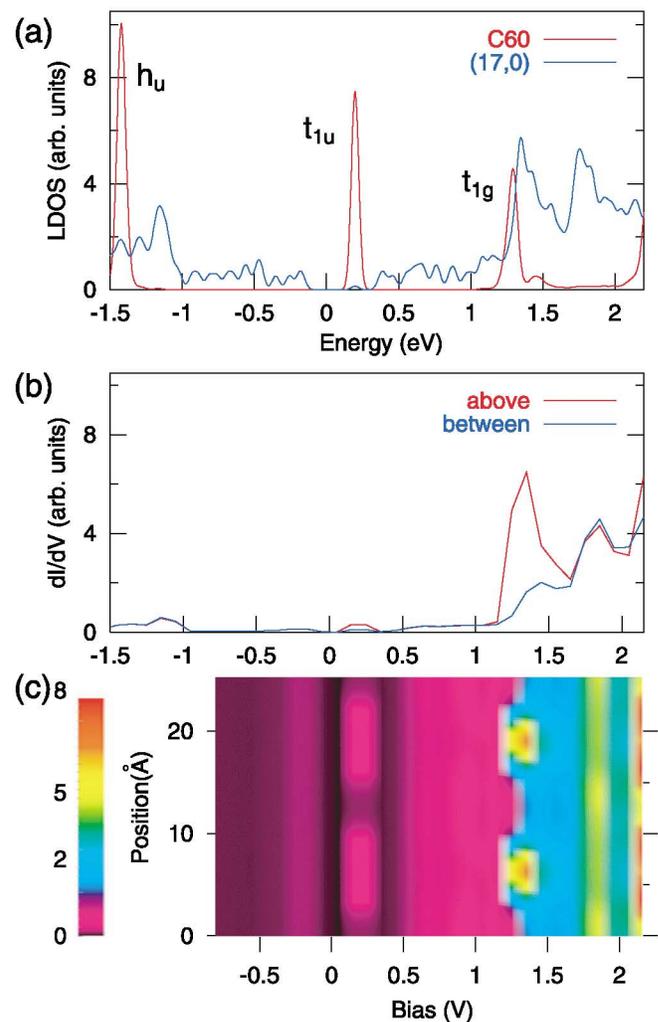
FIG. 2 (color). (a) Local density of states (LDOS) of $C_{60}@(17,0)$ decomposed into the constituents. (b) Simulated dI/dV spectra of $C_{60}@(17,0)$ at two distinct locations, above the center of C_{60} (red) and between two C_{60}'s (blue). Unlike in (a), the DOS is projected onto the plane at 5 Å above the tube wall. (c) Two-dimensional map of the simulated dI/dV spectra as a function of the bias voltage (abscissa) and the position of the tip along the nanotube axis (ordinate).

FIG. 1. Topographic STM image of $C_{60}@(17,0)$ simulated by projecting $\int_{E_f}^{E_f+eV} D(E,\vec{r})dE$ onto the plane at 5 Å above the tube wall where $D(E,\vec{r})$ is the local density of states. (a) Model of $C_{60}@(17,0)$. (b) STM image for −1.5 V sample bias, and (c) the same image for +1.5 V sample bias.

at ~ 1.2 eV at the position above C_{60} but the peak structure is not seen at the position between C_{60}'s, in agreement with Ref. [4]. In Fig. 2(c), more extensive data are presented as a function of the bias voltage (abscissa) and the position along the nanotube axis (ordinate). This compares favorably with the corresponding STS image in Fig. 3A of Ref. [4]. However, the assignment of the peak structure to the electronic level is at variance with the analysis provided there; the peak spots observed around $+1.2$ eV in the STS is associated with the LUMO + 1 of C_{60} with the t_{1g} symmetry instead of the LUMO with the t_{1u} symmetry as assigned in Ref. [4]. The LUMO of C_{60} is located in the middle of the CNT gap according to the present calculation, and we suppose that it evades the STS probe of Ref. [4] in this small-bias range (partly because its tunneling probability is too small). Other than the new assignment of the LUMO + 1 in place of the LUMO to the peak at ~ 1.2 eV, the analysis in Ref. [4] mostly agrees with the present first-principles calculations.

Next, we present the electronic structure of $C_{82}@(17,0)$ and $La@C_{82}@(17,0)$ in order to explain another STS experiment by Lee *et al.* for sparsely packed $Gd@C_{82}$'s inside the CNT [5]. Here, the band gap changes spatially from 0.17 to 0.43 eV as the STM tip moves away from the $Gd@C_{82}$ along the z (tube axis) direction. As mentioned before, Gd in the experiment is replaced by La in the present calculation for the computational purpose. Among nine different low-energy isomers of C_{82}, we choose the one with C_{2V} symmetry since it is known to be most stable when the rare-earth atom is in it [11]. We have considered another isomer with the C_{3V} symmetry which has a comparable stability, but the main results are essentially unchanged. A very long (38 Å) unit supercell in the z direction has been used with the localized basis set [12] when we examine the decay of the C_{82} states.

In Figs. 3(a) and 3(b), the local density of states (LDOS) of $C_{82}@(17,0)$ and $La@C_{82}@(17,0)$ are presented. Note that the low symmetry of C_{82} compared with C_{60} gives rise to several nondegenerate states near the gap region. As C_{82} is packed sparsely inside the nanotube, the direct interfullerene interaction is negligible as in the experiment of Ref. [5]. Comparing (b) with (a), one of the unoccupied C_{82} levels moves down in energy and is half-filled in the presence of La inside. To examine the charge transfer between the CNT and the (metallo)fullerene, we plot the charge transfer $\Delta \rho$ ($= \rho_{\text{peapod}} - \rho_{\text{CNT}} - \rho_{(C_{82}, La@C_{82})}$) in Figs. 3(c) and 3(d). In both cases, the electron transfer occurs from the nanotube to the fullerene and the electrostatic potential energy at the fullerene is raised by ~ 0.4 eV with respect to the nanotube. The amount of the charge transfer is slightly less in (d) than in (c). Three electrons move from La to the fullerene in $La@C_{82}$ before its encapsulation in the nanotube, and a tiny amount of electrons move back to La when $La@C_{82}$ is encapsulated in the nanotube as shown in small red lobes around the La position. Recall that La is located off
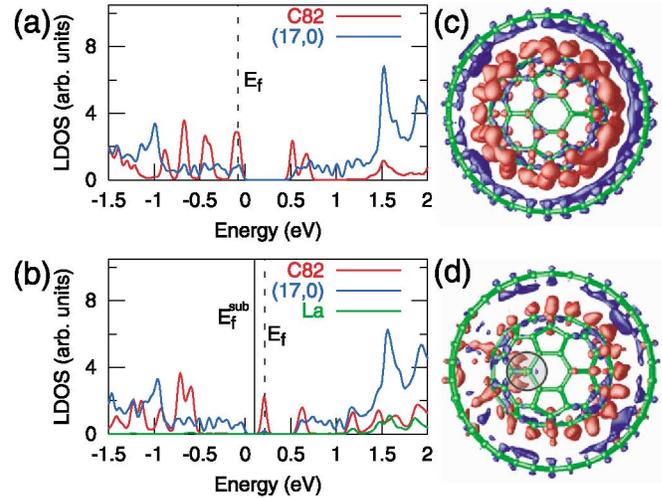
FIG. 3 (color). Local density of states (LDOS) of (a) $C_{82}@(17,0)$ and (b) $La@C_{82}@(17,0)$ decomposed into the constituents. Black vertical lines indicate the Fermi level (E_f). E_f^{sub} represents the Fermi level with the metal substrate in contact. Isodensity surface plots of the electron accumulation (red) and depletion (blue) are shown for $C_{82}@(17,0)$ and $La@C_{82}@(17,0)$ in (c) and (d), respectively. The values for the red and blue surfaces in (c) are $\pm 0.0035 e/\text{Å}^3$. Corresponding values in (d) are $\pm 0.0025 e/\text{Å}^3$. The gray circle in (d) indicates the position of the La atom inside C_{82}.

center of C_{82} (~ 2.5 Å from the hexagonal face of C_{82}), and this leads to the asymmetric distribution of $\Delta \rho$ as shown in Fig. 3(d).

The DOS in Fig. 3 implies that an isolated $La@C_{82}@(17,0)$ would be metallic. In such a case, the metallic substrate in contact with the nanopeapod should be taken into account to describe properly the charged state of the whole system. First-principles calculations on the nanopeapod including the realistic metal substrate are not feasible at present. However, electrons should flow from the peapod to the gold substrate since the work function of the Au(111) substrate (~ 5.3 eV) is greater than that of $La@C_{82}@(17,0)$ (~ 4.8 eV) [13]. From the computed work function of the ionized peapod, we find that two Fermi levels line up when the charge transfer is about one electron per $La@C_{82}$ unit. The new Fermi level of $La@C_{82}@(17,0)$ is within 0.1 eV above the valence band maximum of the CNT as shown by a solid line in Fig. 3(b) and the peapod behaves like a p-type semiconductor. The spatial modulation of the band gap in Ref. [5] then can be explained in terms of the gap between the CNT state (top of its valence band) and the empty $La@C_{82}$ state in the gap of the nanotube. When the STM tip is located right above the C_{82} position (red curve in Fig. 4), the STS is able to pick up the C_{82} states and the effective band gap is ~ 0.2 eV. Because of the strong coupling with the nanotube, the C_{82}-associated peak at ~ 0.1 eV is relatively high compared with the corresponding structure of C_{60} at ~ 0.2 eV in Fig. 2(b). However, the C_{82} state at 0.1 eV is hardly visible between fullerenes
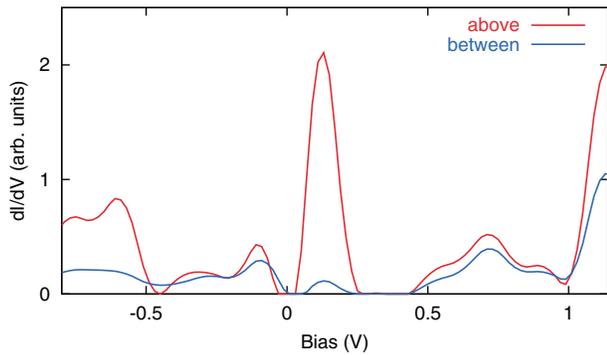
FIG. 4 (color). Simulated dI/dV spectra at two locations as in Fig. 2(b). The zero of energy lies at the Fermi level with the metal substrate in contact. The difference between the two curves is pronounced at bias voltage of 0.1 V, as well as at -0.7 and above 1 V.

(blue) in the dI/dV simulation because the decay length of this state in the z direction is only about 3 Å. Since the interfullerene distance in Ref. [5] is greater than 20 Å, the amplitude of the C_{82} state is too small to be detected when the probing tip is placed midway between two neighboring C_{82}'s. In this case, the detected LUMO is the conduction band minimum of the CNT rather than a C_{82} state and the LDOS recovers the original gap (~ 0.5 eV) of the CNT.

With the charge transfer between the CNT and the gold substrate taken into account as described above, the present calculation indicates that the spatial modulation of the energy level occurs mostly in the LUMO of the system while the valence band maximum is more or less fixed within 0.1 eV below the Fermi level, consistent with experiment. This kind of gap modulation could not be resolved for a densely packed peapod such as in Ref. [4] where the nearest C-C distance between two fullerenes was only ~ 3.4 Å. We note that our calculation shows a rather abrupt change in the gap along the z axis while the real experiment indicates a more continuous modulation. This remaining question is yet to be answered in the future study with more realistic calculations including the substrate as a charge reservoir.

To reinforce the above interpretation of the experimental STS data, we investigate other effects such as strain and the applied electric field. As previously mentioned, there is up to 1% strain on the bonds of the tube for $C_{82}@(17, 0)$ with or without a metal atom inside. The computation for the as-strained $(17, 0)$ nanotube (without the fullerene) to isolate the pure strain effect on the tube band gap indicates that the band gap of the tube actually *increases* by 0.1 eV, as opposed to the observed decrease by 0.3 eV at C_{82} encapsulation sites. For the chiral $(11, 9)$ nanotube with which the experiment in Ref. [5] was done, the band gap change by the strain is estimated to be even smaller ($\lesssim 0.02$ eV). This shows that the strain is not a direct cause of the band gap modulation observed in experiment. We have also simulated the effect of the STM

electric field by including the applied field of 0.1 eV/Å perpendicular to the tube axis, and found no appreciable change in the DOS of the peapod. This is not surprising because the electric field is mostly screened by the peapod and the voltage drop predominantly occurs in the vacuum between the tip and the peapod, rather than within the peapod.

In summary, we have studied the electronic properties of various carbon nanopeapod systems: $C_{60}@(17, 0)$, $C_{82}@(17, 0)$, and $La@C_{82}@(17, 0)$. The orbital hybridization between the LUMO + 1 of C_{60} and the CNT states explains the dominant peak structures observed in the STS measurement. For the strained CNT with sparsely packed $Gd@C_{82}$'s inside, the spatial modulation in the energy gap is well accounted for by the charge transfer and the subsequent shift of the energy levels of the states associated with the encapsulated fullerene.

*Corresponding author.
 Email address: jihm@snu.ac.kr
[1] S. C. Tsang *et al.*, Nature (London) **372**, 159 (1994); C. Guerret-Plécourt *et al.*, *ibid.* **372**, 761 (1994); P. M. Ajayan *et al.*, *ibid.* **375**, 564 (1995); D. Ugarte, A. Chatelain, and W. A. de Heer, Science **274**, 1897 (1996).
[2] B. W. Smith, M. Monthioux, and D. E. Luzzi, Nature (London) **396**, 323 (1998); K. Suenaga *et al.*, Science **290**, 2280 (2000); B. W. Smith, D. E. Luzzi, and Y. Achiba, Chem. Phys. Lett. **331**, 137 (2000); K. Hirahara *et al.*, Phys. Rev. B **64**, 115420 (2001).
[3] S. Okada, S. Saito, and A. Oshiyama, Phys. Rev. Lett. **86**, 3835 (2001).
[4] D. J. Hornbaker *et al.*, Science **295**, 828 (2002).
[5] J. Lee *et al.*, Nature (London) **415**, 1005 (2002).
[6] J. Ihm, A. Zunger, and M. L. Cohen, J. Phys. C **12**, 4409 (1979); J. P. Perdew and A. Zunger, Phys. Rev. B **23**, 5048 (1981).
[7] D. Vanderbilt, Phys. Rev. B **41**, 7892 (1990).
[8] K. Laasonen, W. Andreoni, and M. Parrinello, Science **258**, 1916 (1992).
[9] J. Tersoff and D. R. Hamann, Phys. Rev. B **31**, 805 (1985).
[10] To mimic the finite resolution of the probing tip, the local density of states is averaged over the 1.5 Å-radius circle perpendicular to the tip direction.
[11] K. Kobayashi and S. Nagase, Chem. Phys. Lett. **282**, 325 (1998); E. Nishibori *et al.*, *ibid.* **330**, 497 (2000).
[12] O. F. Sankey and D. J. Niklewski, Phys. Rev. B **40**, 3979 (1989).
[13] Jeroen W. G. Wildöer *et al.*, Nature (London) **391**, 59 (1998).
[14] S. Baroni, A. Dal Corso, S. de Gironcoli, and P. Giannozzi, http://www.pwscf.org.